Journal of Vacuum Science & Technology A

Type-II Band Alignment for Atomic Layer Deposited $HfSiO_4$ on α-Ga_2O_3

Running title: Type-II Band Alignment for $HfSiO_4$ on α-Ga_2O_3

Running Authors: Xia et al.

Xinyi Xia[1], Jian-Sian Li [1], Zhuoqun Wen [2], Kamruzzaman Khan[2], Md Irfan Khan[3], Elaheh Ahmadi[3], Yuichi Oshima[4], David C. Hays[5], Fan Ren[1] and S.J. Pearton[6a)]

[1] Department of Chemical Engineering, University of Florida, Gainesville, FL 32611 USA
[2] Department of Materials Science and Engineering, University of Michigan, Ann Arbor, MI 48109 USA
[3] Department of Electrical Engineering and Computer Science, University of Michigan, Ann Arbor, MI 48109 USA
[4] Optical Single Crystals Group, National Institute for Materials Science, 1-1 Namiki, 305-0044 Tsukuba, Japan
[5] Nanoscale Research Facility, University of Florida, Gainesville, FL 32611 USA
[6] Department of Materials Science and Engineering, University of Florida, Gainesville, FL 32611 USA

[a)] Electronic mail: spear@mse.ufl.edu

There is increasing interest in α-polytype Ga_2O_3 for power device applications, but there are few published reports on dielectrics for this material. Finding a dielectric with large band offsets for both valence and conduction bands is especially challenging given its large bandgap of 5.1eV. One option is $HfSiO_4$ deposited by Atomic Layer Deposition (ALD), which provides conformal, low damage deposition and has a bandgap of 7 eV. The valence band offset of the $HfSiO_4/Ga_2O_3$ heterointerface was measured using X-Ray Photoelectron Spectroscopy. The single-crystal α-Ga_2O_3 was grown by Halide Vapor Phase Epitaxy on sapphire substrates. The valence band offset was 0.82 eV ± 0.20 eV (staggered gap, type II alignment) for ALD $HfSiO_4$ on α-$Ga_{0.2}O_3$. The corresponding

conduction band offset was -2.72 ± 0.45 eV, providing no barrier to electrons moving into the Ga_2O_3.

I. INTRODUCTION

There is significant interest in power device applications of metastable corundum α-Ga_2O_3 due to its even larger bandgap than the stable β-polymorph and the ability to grow it on large area, inexpensive, isomorphous sapphire (α-Al_2O_3) substrates [1-29]. In terms of thermal stability, epitaxial films of α-polytype Ga_2O_3 grown on m-plane sapphire are stable up to 600 °C, allowing significant opportunity for practical device fabrication [25]. This metastable polymorph is found to convert to the β-phase after annealing at 800 °C [29]. Alloying to form α-$(Al_xGa_{1-x})_2O_3$ allows varying the bandgap up to 8.6 eV. This has huge potential for increasing breakdown voltage for power electronics and should be even more radiation-hard against displacement damage than α-Ga_2O_3 due to the higher average bond strength. The current crystal growth issues include lattice mismatch and reduction of defect concentrations [30-33].

Development of dielectrics for α-Ga_2O_3 is challenging due to the large bandgap, which limits the choice of options [34]. A starting point is that the dielectric should have a band gap of at least 2 eV larger given the general rule of thumb of desirably having 1 eV offset in both conduction and valence bands [34-40]. One candidate is $HfSiO_4$, with a bandgap of ~7eV. This has advantages in terms of the large dielectric constant of HfO_2 and the wide bandgap of SiO_2. It is typical to use alternating layers of these dielectrics to form $HfSiO_4$ [39,40]. $HfSiO_4$ has an advantage over pure SiO_2 because of its larger dielectric constant. This allows for use of thicker dielectrics while maintaining an equivalent capacitance to lower dielectric constant materials and has

advantages in MOS device performance. Additionally, by altering the HfO_2:SiO_2 ratio, the bandgap and dielectric constant can be tuned for $Hf_{1-x}Si_xO_4$ [39]. With selection of a gate dielectric, as discussed above, generally at least a 1 eV difference between the insulating material on the gated area and the channel semiconductor is preferred for performance, as that difference will provide a sufficient energy barrier to hole and electron leakage current. In terms of how to deposit the dielectric, Atomic Layer Deposition (ALD) is a preferred option because compared to Physical Vapor Deposition (PVD) methods, it has less disruption to the surface and less chance of contamination [40].

To obtain the band alignment, the standard method is based on precise X-Ray Photoelectron Spectroscopy (XPS) measurement of a core level and the valence band edge for each material investigated and measurement in the shift of the core levels when the two materials have formed the heterojunction [35-38]. The conduction band offset is then obtained from the difference between that and the bandgaps of the dielectric and semiconductor.

In this paper, we report on the determination of the band alignment in the $HfSiO_4$/α-Ga_2O_3 heterostructure, in which the $HfSiO_2$ was deposited by ALD on α-Ga_2O_3 grown by Halide Vapor Phase Epitaxy (HVPE). The valence band offset was obtained from XPS measurements using the Kraut method. The band alignment is type II, staggered gap, meaning the conduction band of the $HfSiO_4$ is above that of the Ga_2O_3 and does not provide electron confinement. The result for $HfSiO_4$ on α-polymorph Ga_2O_3 contrasts with that on β-polymorph, where a type I band alignment with valence band offset of 0.02 eV ± 0.003 eV and a conduction band offset of 2.38 ± 0.50 eV were measured [41].

II. EXPERIMENTAL

The α-Ga_2O_3 layers were grown by halide vapor phase epitaxy on (0001) sapphire substrates at 590°C [42,43]. The growth precursors were O_2 and Ga metal reacted with Hydrochloric acid (HCl) gas to form GaCl and $GaCl_3$. The partial pressures of the precursors were GaCl: 0.25 kPa, O_2: 1.00 kPa and additional HCl: 0.25 kPa, respectively. The additional HCl was supplied to suppress parasitic gas-phase reaction of the precursors by converting a part of GaCl to $GaCl_3$. The carrier gas was N_2. The precursor purities were as follows: Ga metal: > 7N, HCl: > 5N and O_2: > 6.5N. The thicknesses of the α-Ga_2O_3 epilayers were 3-5 μm, and the growth rate was ~28 μm/h. Figure 1 shows an atomic force microscopy (AFM) scan over 5μm × 5μm of the α-Ga_2O_3. This height profile was in a range of ± 8.0nm. The root mean square (RMS) surface roughness was measured to be 3.71nm. The 2Θ-Ω X-ray data from the films is given in Figure 2, showing the 0006 reflection and its proximity to the corresponding Al_2O_3 reflection from the substrate. The α-Ga_2O_3 10-12 pole figure is shown in Figure 3, confirming the excellent crystal quality of the films [42,43].

The ALD $HfSiO_4$ layers were deposited as described previously [39]. This involved a method of alternating cycles of HfO_2 and SiO_2 deposited at 200°C in a plasma-assisted Cambridge Nano Fiji 200 system onto the α-Ga_2O_3 [34]. Both thick (150 nm) and thin (1.5 nm) layers of the dielectrics were deposited [41]. This enabled measurements of both bandgaps of the dielectric and semiconductor and the change in core levels of the thin dielectric on the α-Ga_2O_3. The Inductively Coupled Plasma source power during ALD was 300 W. We used a continuous power application. We have found

it advantageous to use this remote plasma source mode ALD, which reduces the deleterious effects of contaminants and ion induced damage in the films. The deposition sequence was initiated by deposition of HfO_2 using Tetrakis (dimethylamido) hafnium (IV) and O_2 at a rate of 0.9 A/cycle [34]. The second part of the cycle involved deposition of SiO_2 layers using Tris (dimethylamino) silane and O_2 at a rate of 0.6 A/cycle. To achieve the targeted $Hf_{0.5}Si_{0.5}O_4$ composition, three SiO_2 cycles (1.8 A) were followed by two HfO_2 cycles (1.8 A) to keep the desired 1:1 ratio. A schematic of a heterostructure sample of $HfSiO_4$ deposited on the α-Ga_2O_3 is shown in Figure 4.

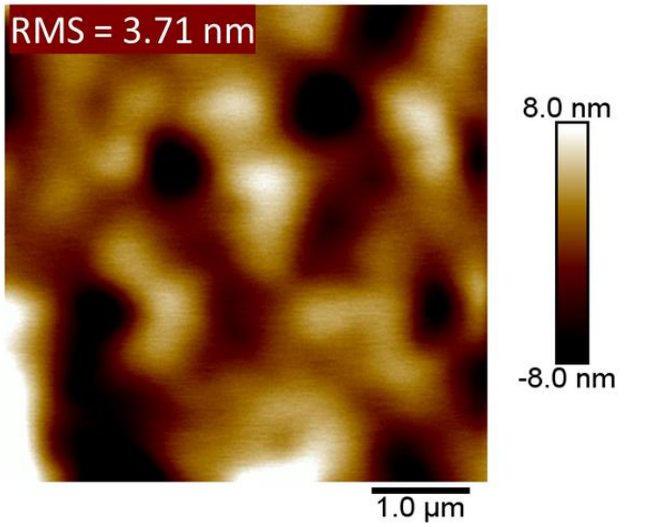

Fig. 1. 5µm × 5µm AFM image of the α-Ga_2O_3. This height profile is in a range of ± 8.0nm. The root mean square (RMS) surface roughness is 3.71nm.

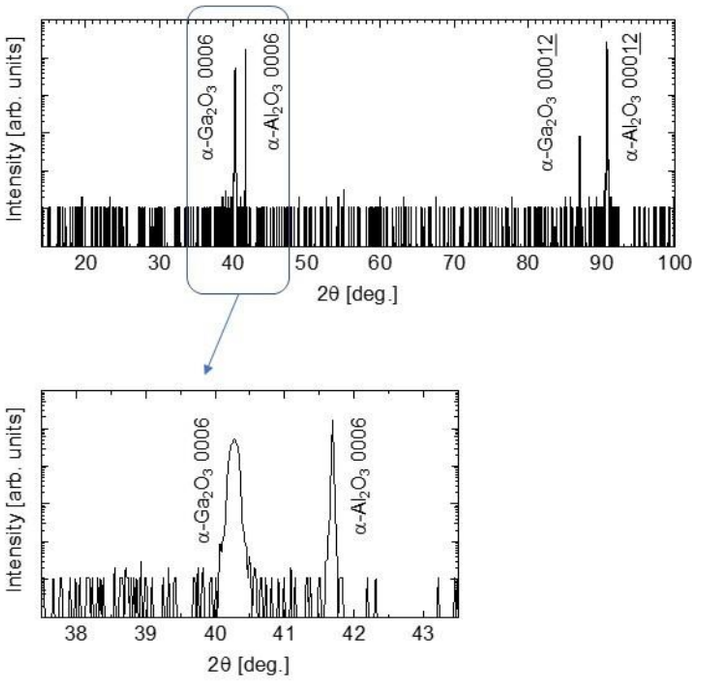

Fig. 2. 2Θ-Ω XRD scan profile from the α-Ga_2O_3 film.

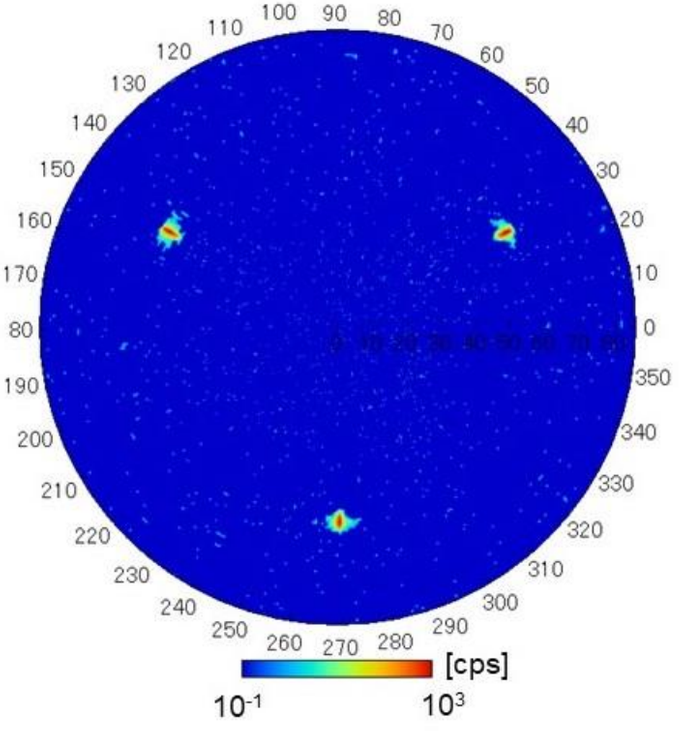

Fig. 3. α-Ga_2O_3 10-12 pole figure from the α-Ga_2O_3 film.

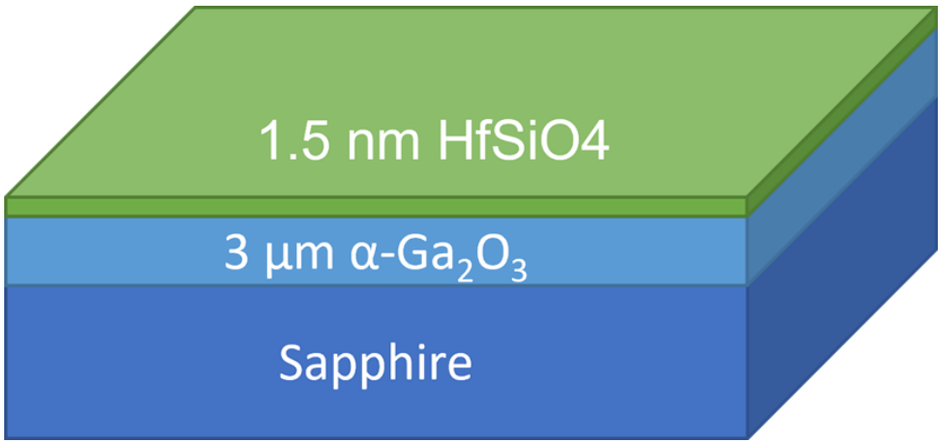

Fig. 4. Schematic of α -Ga_2O_3 epi layer structure used.

The band alignments were determined using the Kraut method [35], based on X-Ray Photoelectron Spectroscopy (XPS) measurements of the shift of core levels and valence band maxima (VBM) in a thick (60 nm) $HfSiO_4$ layer and in the epitaxial α-Ga_2O_3. The shift in these same core level locations (ΔE_{CL}) in the $HfSiO_4$/α-Ga_2O_3 heterojunction allows an accurate determination of the valence band offset (ΔE_V) from [35,40]

$$\Delta E_V = \Delta E_{CL} + (E_{Core} - E_{VBM})_{Ref.\ HfSiO4} - (E_{Core} - E_{VBM})_{Ref.\ Ga_2O_3}$$

XPS measurements were performed on a Physical Instruments ULVAC PHI system. This employs an Al x-ray source (energy 1486.6 eV) with x-ray source power of 300W. The data on all samples was collected from a 100 µm diameter analysis region at a take-off angle of 50° and acceptance angle of ±7 degrees. The electron pass energy was 23.5 eV on high-resolution scans. We estimated the total energy resolution was 0.5 eV, with an accuracy for the binding energies of 0.03 eV. Numerous recent reviews have shown that with adequate precautions [36-38], XPS is the most accurate way of obtaining band alignments and is not subject to the surface and interfacial defect problems that

complicate current or capacitance-based methods [36-38]. We did not observe differential charging and the bandgaps of the $HfSiO_4$ and the α-Ga_2O_3 were consistent with literature values, meaning the determination of valence band offsets is clear-cut.

The bandgap of the α-Ga_2O_3 was obtained using the onset of the plasmon loss feature in O 1s photoemission spectrum. While this technique works well to bandgaps up to ~5 eV, it is less accurate for ultra large bandgap materials and for obtaining the bandgap of the $HfSiO_4$, we used the technique of Reflection Electron Energy Loss Spectroscopy (REELS) [34,40]. This enables a direct measurement of bandgap energy from a linear fit to the leading plasmon peak and finding its zero energy with the background. These spectra were obtained with a 1 kV electron beam and hemispherical electron analyzer.

III. RESULTS AND DISCUSSION

From Figure 5, the bandgap of the α-Ga_2O_3 was determined to be 5.1 ± 0.3 eV, from XPS O1s based electron energy plasmon loss measurements. The measured band gap for the $HfSiO_4$ was 7.0 ± 0.35 eV from the REELS [34,39]. Both of these are consistent with literate values [1, 40]. The difference in bandgaps between $HfSiO_4$ and β-Ga_2O_3 is therefore 1.9 eV.

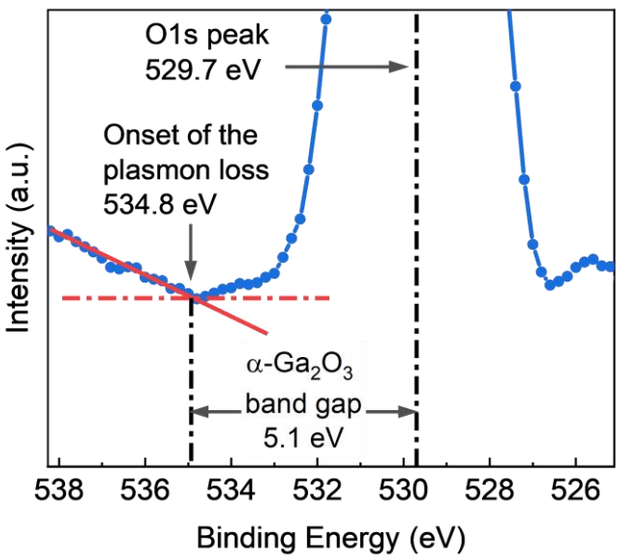

Fig. 5. Bandgap of α-Ga_2O_3 determined using the onset of the plasmon loss feature in O 1s photoemission spectrum.

To determine how this difference is portioned between valence and conduction bands, XPS was performed. XPS survey scans of the three different sample types (α-Ga_2O_3, thick $HfSiO_4$ and the α-Ga_2O_3/$HfSiO_4$ heterostructure) showed the presence of only the lattice constituents. High resolution XPS spectra of the VBM-core delta region are shown in Figure 6 for the α-Ga_2O_3 and Figure 7 shows the XPS spectra for the α-Ga_2O_3 to $HfSiO_4$ core delta regions of the heterostructure samples. These values are summarized in Table I and were then used to calculate ΔEv. The valence band maximum (VBM) was determined by linearly fitting the leading edge of the valence band and the flat energy distribution from the XPS measurements and finding the intersection of these two lines [35,36]. The VBMs were measured to be 3.5 ± 0.2 eV for α-Ga_2O_3 and 3.32 ± 0.4 eV for the $HfSiO_4$.

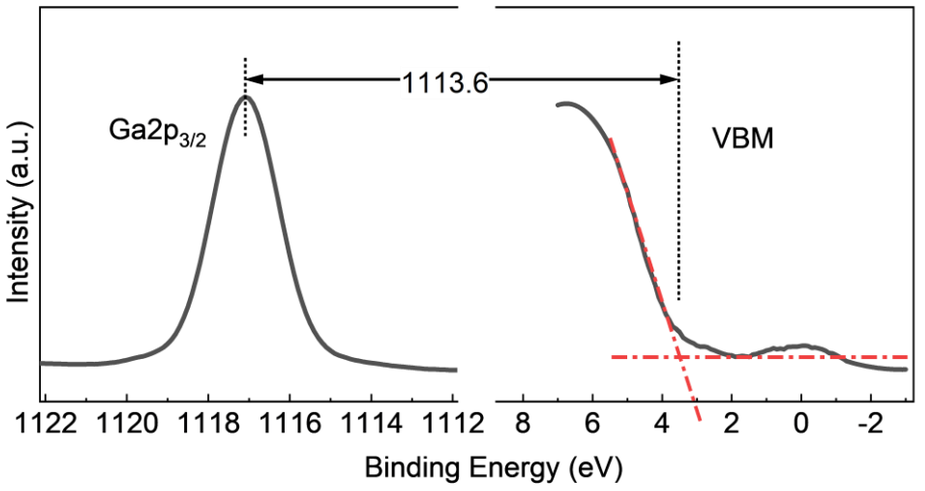

Fig. 6. XPS spectra of core levels to valence band maximum for α-Ga_2O_3.

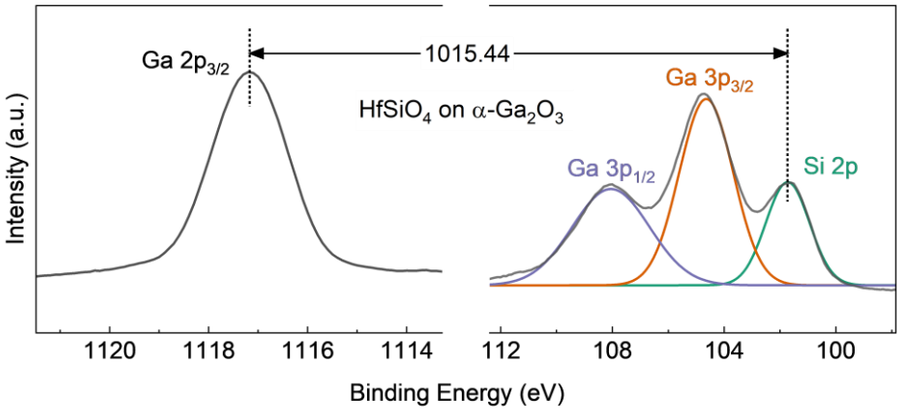

Fig. 7. High resolution XPS spectra for the α-Ga_2O_3 to $HfSiO_4$ core delta regions.

Table I. Valence band maximum and core level data used to calculate the valence band offset of $HfSiO_4$ on α-Ga_2O_3 (eV).

Reference α-Ga_2O_3			
Core Level	VBM	Core Level Peak	Core-VBM
Ga $2p_{3/2}$	3.50	1117.10	1113.60
Reference $HfSiO_4$			
Core Level	VBM	Core Level Peak	Core-VBM
Si 2p	3.32	102.30	98.98
Thin $HfSiO_4$ on α-Ga_2O_3			
Δ Core Level (Ga $2p_{3/2}$ - Si 2p)		Valence Band Offset	
1015.44		0.82	

The band alignment and valence and conduction band offsets were obtained from these core level spectra and are shown in Table 1. It is important to use a well-defined core level since the offsets are small compared to the core level energy and more deviation is expected at higher core level energies.

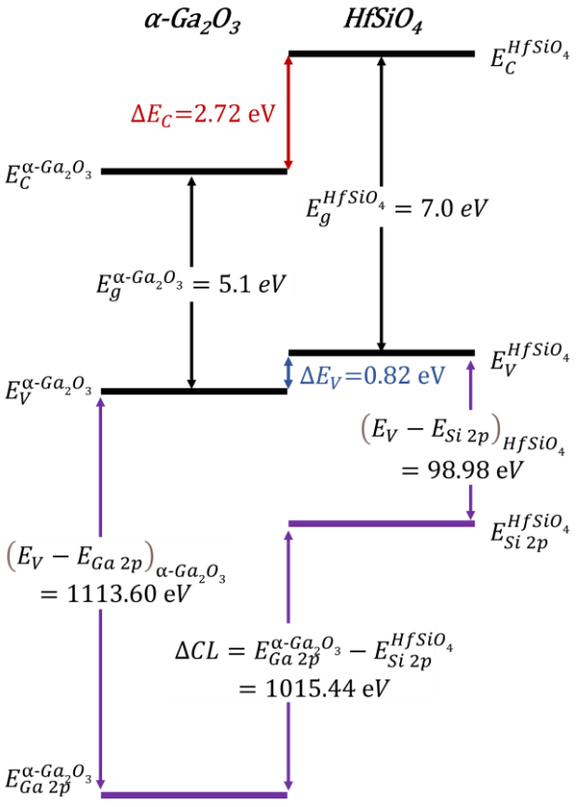

Fig. 8. Band diagrams for the HfSiO4 /α-Ga_2O_3 heterostructure in which the $HfSiO_4$ was deposited by ALD. The valence band offset was determined to be 0.82 eV for ALD $HfSiO_4$ on α-Ga_2O_3. The conduction band offset was 2.72 eV.

Figure 8 shows the extracted band alignment of the $HfSiO_4$/α-$Ga_{0.86})_2O_3$ heterostructure. This is a staggered gap, type II system with a valence band offset of 0.82 ± 0.20 eV and conduction band offset of -2.72 ± 0.45 eV. The valence band offset is smaller than the 1 eV magnitude discussed earlier, so that hole confinement would be less efficient than desired. The negative conduction band offset means there is no electron confinement at all, with the band alignment actually conducive to electron injection. The corresponding values for the $HfSiO_4$/β-Ga_2O_3 are $\Delta E_V = 0.02eV$ and $\Delta E = 2.38eV$.[34] The results for the alpha polytype are in contrast to β-Ga_2O_3, where $HfSiO_4$ provides

good electron confinement, but essentially no hole confinement. $HfSiO_4$ is still an option for surface passivation of α-GaO_3.

IV. SUMMARY AND CONCLUSIONS

The band alignment at $HfSiO_4$/ α-$Ga_{02}O_3$ heterojunctions is a staggered gap (type II. The valence band offset was 0.82 ± 0.20 eV and the conduction band offset was -2.72 ± 0.45 eV. The conduction band offset does not provide any electron confinement, while even the valence band offset is marginal for hole confinement. Since the dielectric constant of the $HfSiO_4$ is attractive compared to some alternatives, it could still be a component in in multi-level gate stacks on transistor structures to increase the capacitance. It could also be a suitable candidate as a surface passivation layer to protect the α-Ga_2O_3. There have not yet been detailed published studies on the sensitivity of the α-Ga_2O_3 surface to environmental exposure or processing steps, but results from the β-polytype shows that such protection is needed [44,45].

ACKNOWLEDGMENTS

The authors would like to thank the Research Service Center (RSC) staff at the University of Florida for their help in the fabrication and characterization of these materials. The work at UF was performed as part of Interaction of Ionizing Radiation with Matter University Research Alliance (IIRM-URA), sponsored by the Department of the Defense, Defense Threat Reduction Agency under award HDTRA1-20-2-0002. The content of the information does not necessarily reflect the position or the policy of the federal government, and no official endorsement should be inferred. The work at UF was

also supported by NSF DMR 1856662 (James Edgar). The work at UMichigan was supported by Naval Research Office under Contract N00014-19-1-2225.

The authors would like to thank Cindy Lee for the AFM and XRD.

AUTHOR DECLARATIONS

The authors have no conflicts to disclose.

DATA AVAILABILITY

All data that support the findings of this study are included within the article.

REFERENCES

[1]E. Ahmadi and Y. Oshima, J. Appl. Phys. **126**, 160901 (2019).

[2]Takuya Maeda, Mitsuru Okigawa, Yuji Kato, Isao Takahashi, and Takashi Shinohe, AIP Adv. **10**, 125119 (2020).

[3]A. Hassa, P. Storm, M. Kneiß, D. Splith, H. von Wenckstern, M. Lorenz and M. Grundmann, Phys. Stat. Solidi B, **258**, 2000394 (2021).

[4]H. Zhang, L. Yuan, X. Tang, J. Hu, J. Sun, Y. Zhang, Y. Zhang, and R. Jia, IEEE T Power Electr. **35**, 5157 (2020).

[5]A. Y. Polyakov, V. I. Nikolaev, E. B. Yakimov, F. Ren, S. J. Pearton, and J. Kim, J. Vac. Sci. Technol. A **40**, 020804 (2022).

[6]Zhengpeng Wang, Xuanhu Chen, Fang-Fang Ren, Shulin Gu and Jiandong Ye, J. Phys D: Appl Phys, **54**, 043002 (2021).

[7]I. Cora, Z. Fogarassy, R. Fornari, M. Bosi, A. Rečnik, and B. Pecz, Acta Mater.**183**, 216 (2020).

[8]A. F. M. A. U. Bhuiyan, Z. Feng, J. M. Johnson, H.-L. Huang, J. Sarker, M. Zhu, M. R. Karim, B. Mazumder, J. Hwang, and H. Zhao, APL Mater. **8**, 031104 (2020).

[9]M. Hilfiker, U. Kilic, M. Stokey, R. Jinno, Y. Cho, H. G. Xing, D. Jena, R. Korlacki, and M. Schubert, Appl. Phys. Lett. **119**, 092103 (2021).

[10]K. Uno, R. Jinno, and S. Fujita, J. Appl. Phys. **131**, 090902 (2022).

[11]J. A. Spencer, A. L. Mock, A. G. Jacobs, M. Schubert, Y. Zhang, and M. J. Tadjer, Appl. Phys. Rev. **9**, 011315 (2022).

[12]Y. J. Zhang, Z. P. Wang, Y. Kuang, H. H. Gong, J. G. Hao, X. Y. Sun, F.-F. Ren, Y. Yang, S. L. Gu, Y. D. Zheng, R. Zhang, and J. D. Ye, Appl. Phys. Lett. **120**, 121601 (2022).

[13]D. Yang, B. Kim, T. H. Eom, Y. Park, and H. W. Jang, Electron. Mater. Lett.**18**, 113 (2022).

[14]Andrew Venzie, Amanda Portoff, Michael Stavola, W. Beall Fowler, Jihyun Kim, Dae-Woo Jeon, Ji-Hyeon Park, and Stephen J. Pearton, Appl. Phys. Lett. **120**, 192101 (2022).

[15]R. Schewski, G. Wagner, M. Baldini, D. Gogova, Z. Galazka, T. Schulz, T. Remmele, T. Markurt, H. von Wenckstern, M. Grundmann, O. Bierwagen, P. Vogt, and M. Albrecht, Appl. Phys. Express **8**, 011101 (2015).

[16]M. Kracht, A. Karg, M. Feneberg, J. Bläsing, J. Schörmann, R. Goldhahn, and M. Eickhoff, Phys. Rev. Appl. **10**, 024047 (2018).

[17]A. Polyakov, V. Nikolaev, S. Stepanov, A. Almaev, A. Pechnikov, E. Yakimov, B. O. Kushnarev, I. Shchemerov, M. Scheglov, A. Chernykh, A. Vasilev, A. Kochkova, and S. J. Pearton J. Appl. Phys. **131**, 215701 (2022).

[18]Y. Oshima, K. Kawara, T. Shinohe, T. Hitora, M. Kasu, and S. Fujita, APL Mater. **7**, 022503 (2019).

[19]Matthew Hilfiker, Rafał Korlacki, Riena Jinno, Yongjin Cho, Huili Grace Xing, Debdeep Jena, Ufuk Kilic, Megan Stokey, Mathias Schubert, Appl. Phys. Lett, **118**, 6, (062103), (2021).

[20]V.I. Nikolaev A.Y. Polyakov, S.I. Stepanov, A.I. Pechnikov, E.B. Yakimov, A.V. Chernykh, A.A. Vasilev, I.V. Shchemerov, A.I. Kochkova, L. Guzilova, M.P. Konovalov and S.J. Pearton, ECS J. Solid State Sci. Technol. **11**, 115002 (2022).

[21]K. Kawara, Y. Oshima, M. Okigawa, and T. Shinohe, Appl. Phys. Express **13**, 075507 (2020).

[22]Andrew Venzie, Amanda Portoff, W. Beall Fowler, Michael Stavola, Dae Woo Jeon, Jihyun Kim and S. J. Pearton, Appl. Phys. Lett. **120**, 192101 (2022).

[23]Alexander Y. Polyakov, Vladimir I. Nikolaev, Igor N. Meshkov, Krzysztof Siemek, Petr B. Lagov, Eugene B. Yakimov, Alexei I. Pechnikov, Oleg S. Orlov, Alexey A. Sidorin, Sergey I. Stepanov, Ivan V. Shchemerov, Anton A. Vasilev, Alexey V. Chernykh, Anton A. Losev, Alexandr D. Miliachenko, Igor A. Khrisanov, Yu.S. Pavlov, U.A. Kobets and S. J. Pearton, J. Appl. Phys. **132**, 035701 (2022).

[24]A. Sharma and U. Singisetti, Appl. Phys. Lett. **118**, 032101 (2021).

[25]Riena Jinno, Kentaro Kaneko and Shizuo Fujita, Jpn. J. Appl. Phys, **60**, SB, (SBBD13), (2021).

[26]A. Segura, L. Artus, R. Cusco, R. Goldhahn, and M. Feneberg, Phys. Rev. Mater. **1**, 024604 (2017).

[27]M. Hilfiker, R. Korlacki, R. Jinno, Y. Cho, H. G. Xing, D. Jena, U. Kilic,M. Stokey, and M. Schubert, Appl. Phys. Lett. **118**, 062103 (2021).

[28]M. Feneberg, J. Nixdorf, M. D. Neumann, N. Esser, L. Artus, R. Cusco, T. Yamaguchi, and R. Goldhahn, Phys. Rev. Mater. **2**, 044601 (2018).

[29]M. Stokey, R. Korlacki, M. Hilfiker, S. Knight, S. Richter, V. Darakchieva, R. Jinno, Y. Cho, G. H. Xing, D. Jena, Y. Oshima, K. Khan, E. Ahmadi, and M. Schubert, Phys. Rev. Mater. **6**, 014601 (2022).

[30]A. Y. Polyakov, N. B. Smirnov, I. V. Shchemerov, E. B. Yakimov, V. I. Nikolaev, S. I. Stepanov, A. I. Pechnikov, A. V. Chernykh, K. D. Shcherbachev, A. S. Shikoh, A. Kochkova, A. A. Vasilev, and S. J. Pearton, APL Materials **7**, 051103 (2019)

[31]S. I. Kan, S. Takemoto, K. Kaneko, I. Takahashi, M. Sugimoto, and T. Shinohe, Appl. Phys. Lett. **113**, 212104 (2018).

[32]J. G. Hao, H. H. Gong, X. H. Chen, Y. Xu, F. F. Ren, and S. L. Gu, Appl. Phys. Lett. **118**, 261601 (2021).

[33]J. P. McCandless, C. S. Chang, K. Nomoto, J. Casamento, V. Protasenko, P. Vogt, D. Rowe, K. Gann, S. T. Ho, W. Li, R. Jinno, Y. Cho, A. J. Green, K. D. Chabak, D. G.

Schlom, M. O. Thompson, D. A. Muller, H. G. Xing, and D. Jena, Appl. Phys. Lett. **119**, 062102 (2021).

[34]Patrick H. Carey, Fan Ren, David C. Hays, Brent P. Gila, Stephen J. Pearton, Soohwan Jang and Akito Kuramata, Jpn. J. Appl. Phys. 56, 071101 (2017).

[35]E. A. Kraut, R. W. Grant, J. R. Waldrop, and S. P. Kowalczyk, Phys. Rev. Lett., **44**, 1620 (1980).

[36]Scott A. Chambers, Le Wang, and Donald R. Baer, J. Vac. Sci Technol A **38**, 061201 (2020).

[37]Grzegorz Greczynski and Lars Hultman, J. Appl. Phys. 132, 011101 (2022).

[38]Grzegorz Greczynski, Lars Hultman, Science Talks 1, 100007 (2022).

[39]C. Fares, F. Ren, Max Knessl, H. von Wenckstern, M. Grundmann and S.J. Pearton, chapter 9 in Wide Bandgap Semiconductor Based Electronics, ed F. Ren and S.J. Pearton (IOP Publishing, Bristol, (2020).

[40]D. C. Hays, B.P. Gila, S. J. Pearton and F. Ren, Appl. Phys. Rev.,**4**, 021301 (2017).

[41]Xinyi Xia, Nahid Sultan Al Mamun, Maxwell Wetherington, Fan Ren, Aman Haque and S.J. Pearton, J. Vac. Sci. Technol. A 40, 053403 (2022).

[42]Yuichi Oshima, Katsuaki Kawara, Takayoshi Oshima, Mitsuru Okigawa and Takashi Shinohe, Semicond. Sci. Technol. **35**, 055022 (2020).

[43]Yuichi Oshima, Encarnación G. Víllora, and Kiyoshi Shimamura, Appl. Phys. Expr. **8**, 055501 (2015).

[44]J. Kim, F. Ren and S.J. Pearton, Nanoscale Horizons **4**, 1251(2019).

[45]J. E. N. Swallow, J. B. Varley, L. A. H. Jones, J. T. Gibbon, L. F. J. Piper, V. R. Dhanak, and T. D. Veal, APL Materials **7**, 022528 (2019).

Journal of Vacuum Science & Technology A

PLEASE CITE THIS ARTICLE AS DOI: 10.1116/6.0002453

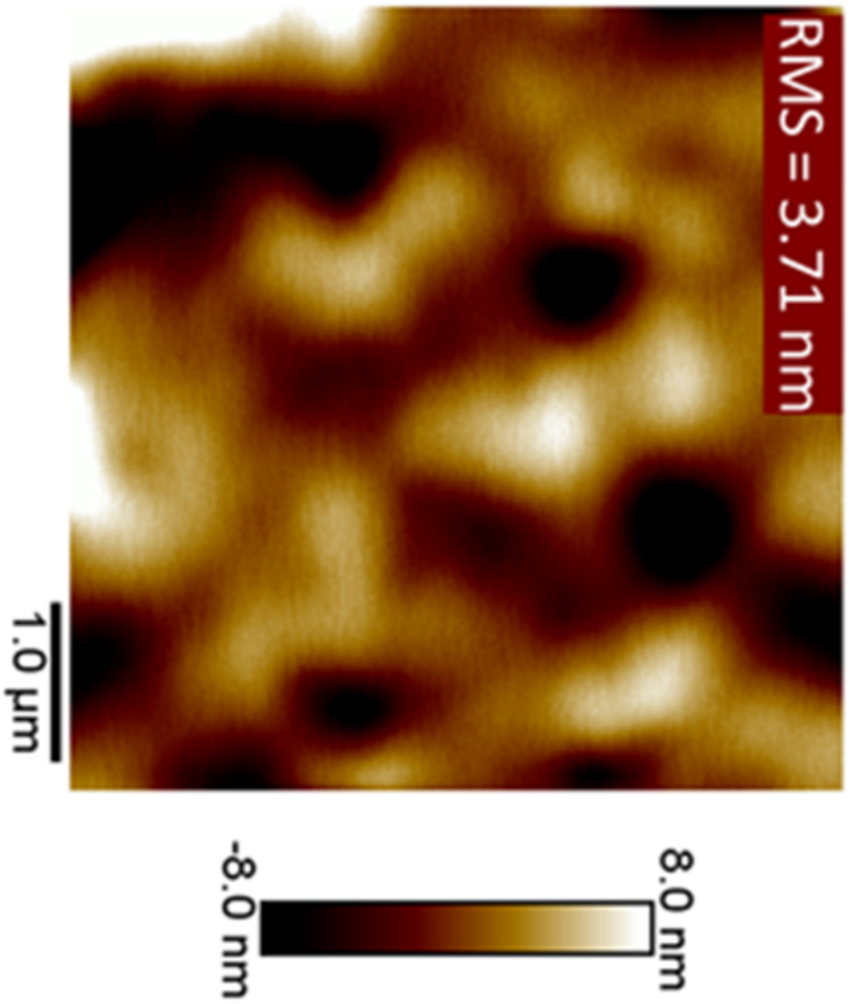

Journal of Vacuum Science & Technology A

PLEASE CITE THIS ARTICLE AS DOI: 10.1116/6.0002453

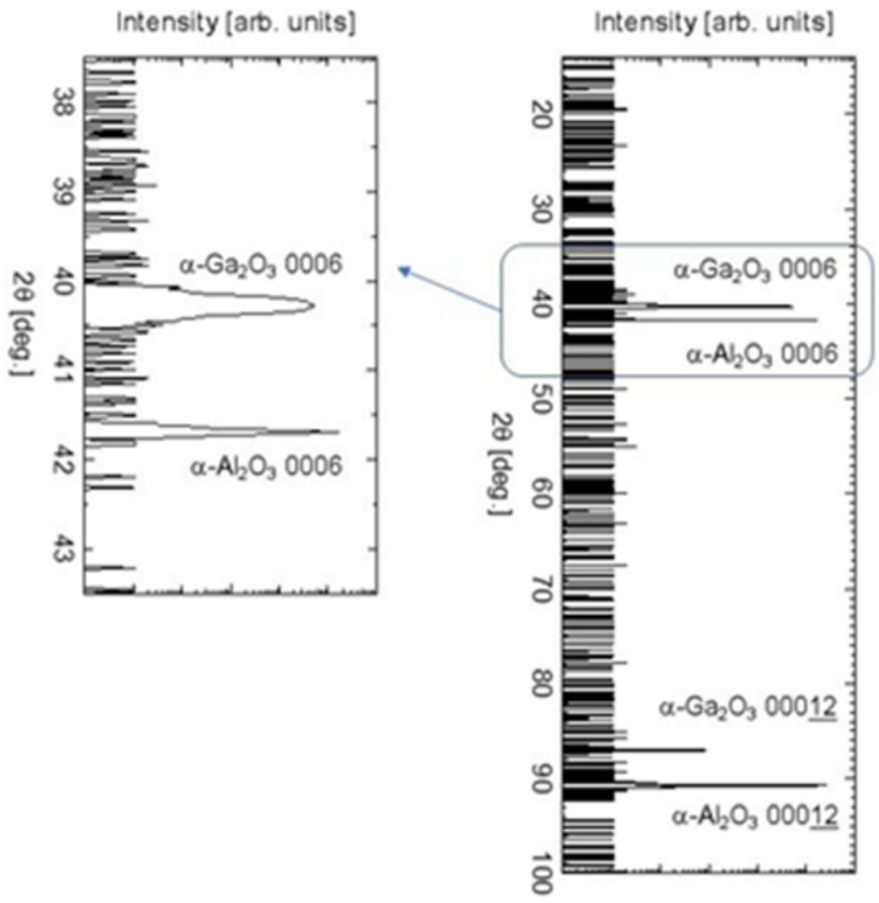

Journal of Vacuum Science & Technology A

PLEASE CITE THIS ARTICLE AS DOI: 10.1116/6.0002453

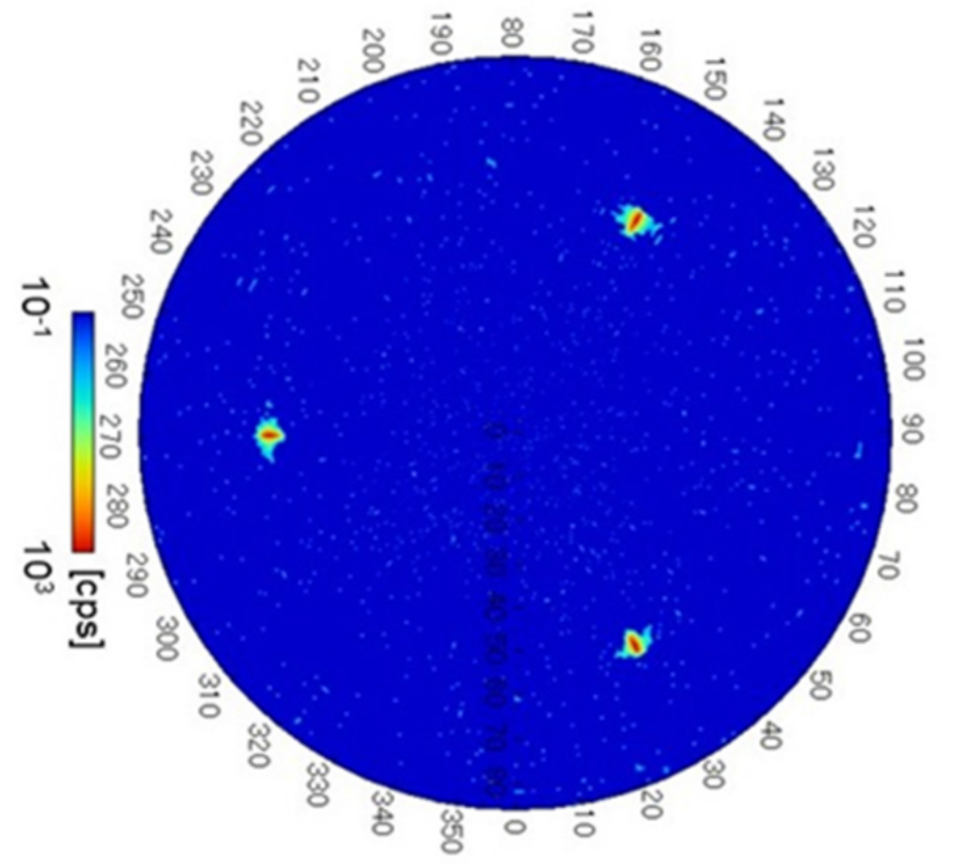

Journal of Vacuum Science & Technology A

PLEASE CITE THIS ARTICLE AS DOI: 10.1116/6.0002453

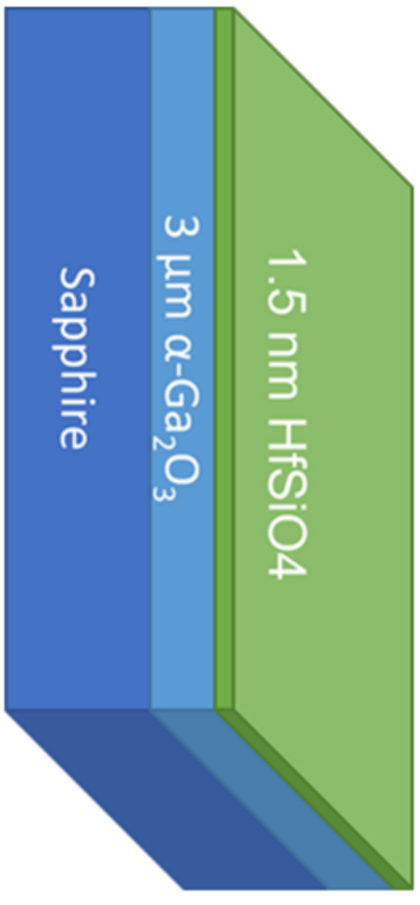

Journal of Vacuum Science & Technology A

PLEASE CITE THIS ARTICLE AS DOI: 10.1116/6.0002453

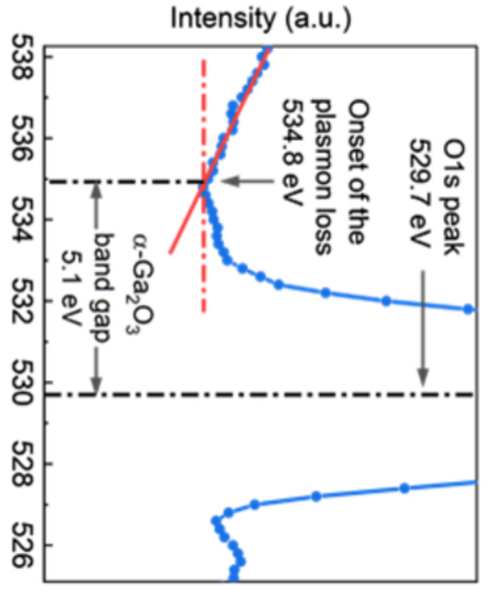

Journal of Vacuum Science & Technology A

PLEASE CITE THIS ARTICLE AS DOI: 10.1116/6.0002453

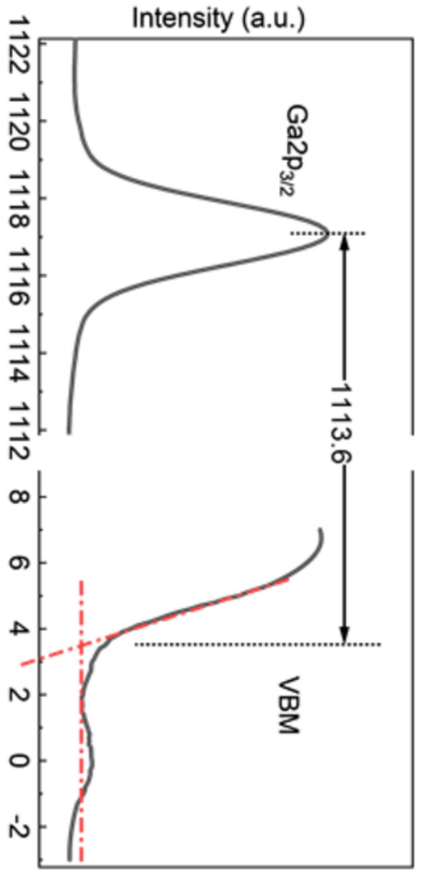

Journal of Vacuum Science & Technology A

PLEASE CITE THIS ARTICLE AS DOI: 10.1116/6.0002453

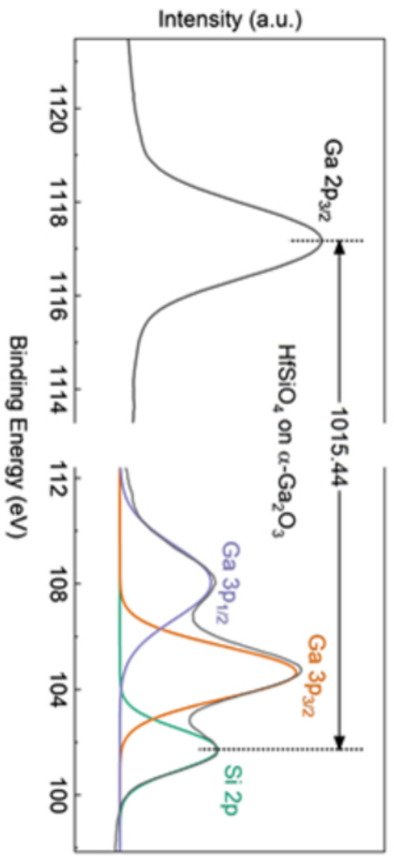

Journal of Vacuum Science & Technology A

ACCEPTED MANUSCRIPT

This is the author's peer reviewed, accepted manuscript. However, the online version of record will be different from this version once it has been copyedited and typeset.
PLEASE CITE THIS ARTICLE AS DOI: 10.1116/6.0002453